Received: 3 October 2022 | Revised: 12 May 2023 | Accepted: 21 May 2023

DOI: 10.1002/ldr.4816

RESEARCH ARTICLE

WILEY

Particulate phosphorus in runoff in a Mediterranean agroforestry catchment driven by land use and rainfall characteristics

María Concepción Ramos[1] | Ivan Lizaga[2] | Leticia Gaspar[3] | Ana Navas[3]

[1]Department of Chemistry, Physics and Environmental and Soil Sciences, University of Lleida-Agrotecnio, Lleida, Spain

[2]Department of Green Chemistry and Technology, Isotope Bioscience Laboratory–ISOFYS, Ghent University, Gent, Belgium

[3]Estación Experimental de Aula Dei, EEAD-CSIC, Zaragoza, Spain

Correspondence
María Concepción Ramos, Department of Chemistry, Physics and Environmental and Soil Sciences, University of Lleida-Agrotecnio, Lleida 25198, Spain.
Email: cramos@macs.udl.es

Funding information
Research Foundation-Flanders; Ministerio de Ciencia e Innovación

Abstract

This study examined phosphorus (P) delivery and transport in flood events in an agroforestry catchment, with cropland and forestland as the main land uses. Sediments were collected in artificial-lawn mats (MATs) distributed in five locations across the catchment (MAT1 to MAT5) along 20 seasonal campaigns during 5 years, in which rainfall with different characteristics was recorded. The properties analyzed in the surface soils under different land uses, and in the MATs used for collecting sediments included particle size and other properties such as soil organic matter (SOM), low frequency magnetic susceptibility (χLF) and P and Ti concentrations. The rainfall characteristics of the events recorded in each campaign were analyzed and the campaigns were grouped using cluster analysis taken into account the characteristics of the sediments collected. There was a P enrichment in the sediments compared to the sediment sources. The greatest P concentration was associated to sediment rich in clay and SOM. However, the sediment showed lower χLF, which could be due to higher erosion rates from the most degraded soils. The highest P losses were recorded at the catchment outlet, where the surface occupied by croplands was higher, with P values around 1.3 × times higher than at the headwaters. The differences between monitoring campaigns were attributed to differences in precipitation patterns that influence the hydrological response. The higher P concentration in the sediment during the campaigns that accumulated higher amount of rainfall in shorter periods of time confirmed the direct influence of rainfall intensity on the P mobilization.

KEYWORDS
ephemeral streams, land uses, phosphorus, phosphorus mobilization, rainfall intensity, soil binding

1 | INTRODUCTION

Soil erosion is the main soil degradation process in Mediterranean climate areas, which causes not only soil losses but also the exportation of significant amounts of nutrients out of the catchments. It implies loss of soil fertility and in addition a risk for water quality. The magnitude of soil erosion depends on rainfall and soil characteristics, but land use and its management play also an important role (Da Silva et al., 2017; García-Ruiz, 2010). Rainfall intensity, which is directly linked to the energy that the drop impact has to detach the soil particles, is the most relevant rainfall characteristic in the first phase of the erosion process, while rainfall amount is directly linked to runoff response.

In the last decades, the number of events of high intensity seems to increase (Abbasnia & Toros, 2018; Kharin et al., 2007; Ramos & Durán, 2014; Vallebona et al., 2015) and that increase could be accentuated under climate change projections (Hosseinzadehtalaei et al., 2020; Nadal-Romero et al., 2022). Studies carried out in Mediterranean climate areas indicated that most soil losses by erosion in each year are produced in a reduced number of events of high magnitude (Ramos & Martínez-Casasnovas, 2009) and the more frequent extreme events would increase soil erosion (Nadal-Romero et al., 2022) and channel bank erosion (Gaspar et al., 2019; Lizaga et al., 2019).

Soils rich in fine material, in particular soils rich in silt content, are very susceptible to be eroded (Ramos et al., 2000), and the degree of soil protection in these cases is important to reduce the effect of the drop impact. Forest and vegetated areas offer higher cover degree than croplands, where the soil remains bare during long time periods, making them more prone to erosion processes (Oliveria, et al., 2015). On the other hand, in areas where croplands have been abandoned, the degradation process has increased very rapidly, leaving on top of the surface exposed soils that are very susceptible to be eroded (García-Ruiz & Lana-Renault, 2011).

Among land uses, croplands, due to fertilization practices, tend to have higher nutrient levels, in particular of P, than other land uses, which implies higher potential nutrient sources to water bodies. In fact, croplands are considered dominant nonpoint sources of nutrient to water bodies (Ma et al., 2016) and the proportion of cropland in a catchment has the strongest positive effect on its nutrient concentrations in streams, while increasing proportion of forest and wetland has an opposite effect (Djodjic et al., 2021). Nevertheless, management practices influence the amount of P to be delivered under any land use (Jin et al., 2009; Yuan & Koropeckyj-Cox, 2022).

There is an increasing concern about P levels reaching water bodies from croplands and on the establishment of changes in the management to reduce these loads (Wang et al., 2017). However, croplands are not the only source and all land uses should be considered as potential P sources (Granger et al., 2021) and, under high intensity events, the P contribution from streambeds and riverbanks can be also relevant (Ramos et al., 2022).

In addition, the form in which P is linked to soil particle conditions the total P delivery and exportation (Gérard, 2016; Spohn, 2020). For this reason, the analysis of additional soil properties can help in the understanding of processes. In this respect Ti concentrations and the low frequency magnetic susceptibility (χLF) have been considered among the properties that can provide useful information about the origin of P and on the soil surface changes due to erosion. As Titanium, mainly in form of TiO_2, normally decreases from the soil surface to the bedrock (Kaup & Carter, 1987), some differences can be found in eroded soils. On the other hand, the χLF has been associated to the interaction of factors such as topography, climate or soil properties, among other factors (Magiera et al., 2006) and their values can reflect the intensity of existing processes in different positions of the landscape (Yang et al., 2009), which may vary as a result of erosion processes.

In terms of nutrient losses and exportation, an example of such an area in which the erosion processes can imply a serious concern can be found in a vast band extending at the south of the Pyrenees (Aragón, Spain). In this area, cropland and forestland intermix with areas that, after being cultivated for decades, were abandoned, giving rise to significant changes in land use and cover (Lasanta et al., 2016; Navas et al., 2017). In the region, previous studies have shown the magnitude of the erosion processes and its impact on soil losses (Lizaga et al., 2020; Navas et al., 2014), but less information exists on its effect on P exportation depending on rainfall characteristics. Although the P mobilization in the streams associated to an exceptional event in this particular area was previously analyzed (Ramos et al., 2022), we hypothesize that P dynamics could differ under different rainfalls that generate regular floods. To cover this gap, we focus on fine sediments accumulated in small lateral aggradation bars of a system of ephemeral streams draining an agroforestry catchment after rainfall of regular characteristics during the annual seasons. Although P can be transported by runoff as dissolved and particulate P, we focus on the particulate fraction. Previous studies carried out under simulated rainfall in soils of the area under different land uses/land covers and using different rainfall intensities confirmed that the concentration of dissolved P in the runoff was very low and in many cases negligible compared to the concentration of P associated to soil particles (Ramos et al., 2019). This research tries to assess: (i) the characteristics of interest to understand the behaviour of P in the sediments transported by runoff generated in rainfall events of different characteristics that trigger floods, and (ii) the sediment variability between areas with different predominant land use. The information was recorded in 20 monitoring seasonal campaigns extending from 2014 to 2019, in which rainfall events of different magnitude that produced floods were recorded. The characteristics of the rainfalls as well as of the soils under different land uses and other sediment sources (all of them termed as sources) were evaluated. In addition to P concentration in the sediments, other soil properties such as SOM, the χLF, and Ti concentrations were considered, which together with grain size could give information about the P origin and about the impact of rainfall on soil surface changes due to erosion.

2 | MATERIALS AND METHODS

2.1 | The study area

The research was conducted in a small catchment (843.3 ha) located in the northern border of the Ebro valley, Spain, at elevations between 638.3 and 963.9 m a.s.l. The catchment is drained by a system of small ephemeral streams of which the longest is the Cenera stream that is a tributary of the main catchment previously studied (Ramos et al., 2022). The streams incise the fluvial terraces creating talus of altitudes between 1 m to more than 3 m at the outlet of the Cenera catchment. Streambanks have been found to be very active in supplying sediments during extreme floods (Gaspar et al., 2019) and are also included as sediment source in this study. In the incised streams, sediments accumulate in lateral aggradation bars that have small development only 10–30 cm above the active streambed. During very high floods in some reaches, the small lateral bars can be washed out and fully removed. The main land use/land covers comprise croplands and forest areas that include open forest, afforested areas and scrubs (Lizaga et al., 2018) (Figure 1). The forest and the scrublands occupy the highest altitudes, while the croplands are located at the valley floors and on fluvial terraces on gentle slopes. The afforested lands are at intermediate altitudes, occupying previously cultivated and later abandoned areas. In addition, some areas covered by very degraded soils (barren land) can be found at scattered locations in the catchment. The croplands cover 13.8% of the surface, while the forest areas represent about 82% of the total surface, and the degraded soils represent a small percentage (2.4%). The area has a continental climate, with cold winters and hot and dry summers (average maximum temperatures of about 17°C and average minimum temperatures of about 7°C (https://www.aragon.es/-/atlas-climatico-de-aragon), and with about 550 mm of annual precipitation, which is mainly concentrated in spring and autumn.

2.2 | Characteristics of the sediment sources

The soils of the Cenera catchment were characterized in field surveys as Cambisols (68.9%), Calcisols (1.4%), Leptosols (14.6%), Fluvisols (5.1%) and Regosols (9.9%) (Machin-EEAD-CSIC, personal communication). The characteristics of the soil surface (0–2 cm) were analyzed in a total of 35 points covering all land uses: 10 in croplands and 25 in forest areas (7 in open forest; 13 in afforested areas and 5 in scrublands). In addition, highly degraded soil was sampled at 12 points in barren lands and another 14 points were sampled in streambanks. The distribution of the sampling points is shown in Figure 2.

Soil samples were air-dried, homogenized and sieved to ≤0.063 mm to make the results comparable to those of the fine sediments trapped in the MATs. Particle size analyses (USDA) were performed using a Coulter LS 13320 laser diffraction particle size analyzer (Beckman Coulter, Inc., 2011), after eliminating the organic matter. Soil organic carbon (SOC) was measured on a subsample finely ground via a dry combustion method using a LECO RC-612 multiphase carbon analyzer (LECO Corporation, St. Joseph, MI, USA, LECO, 1996). The SOM was obtained by multiplying soil SOC by the Van Bemmelen conversion factor (1.724). Total P and Ti content were analyzed by ICP, and the χLF was determined using a Bartington susceptibility meter.

2.3 | Sediment characterization

Sediments were collected after flood events using artificial-lawn mats (MATs), placed at different locations within the catchment (1–5) (Figure 2), at accretion sites in lateral bars where the stream energy is reduced and natural deposition can take place.

Samples were collected in 20 seasonal campaigns in the period extending from October/2014 to October/2019. Two replicates were collected in the last 12 periods and the average values were used in further analysis. The trapped sediments were dried and sieved to

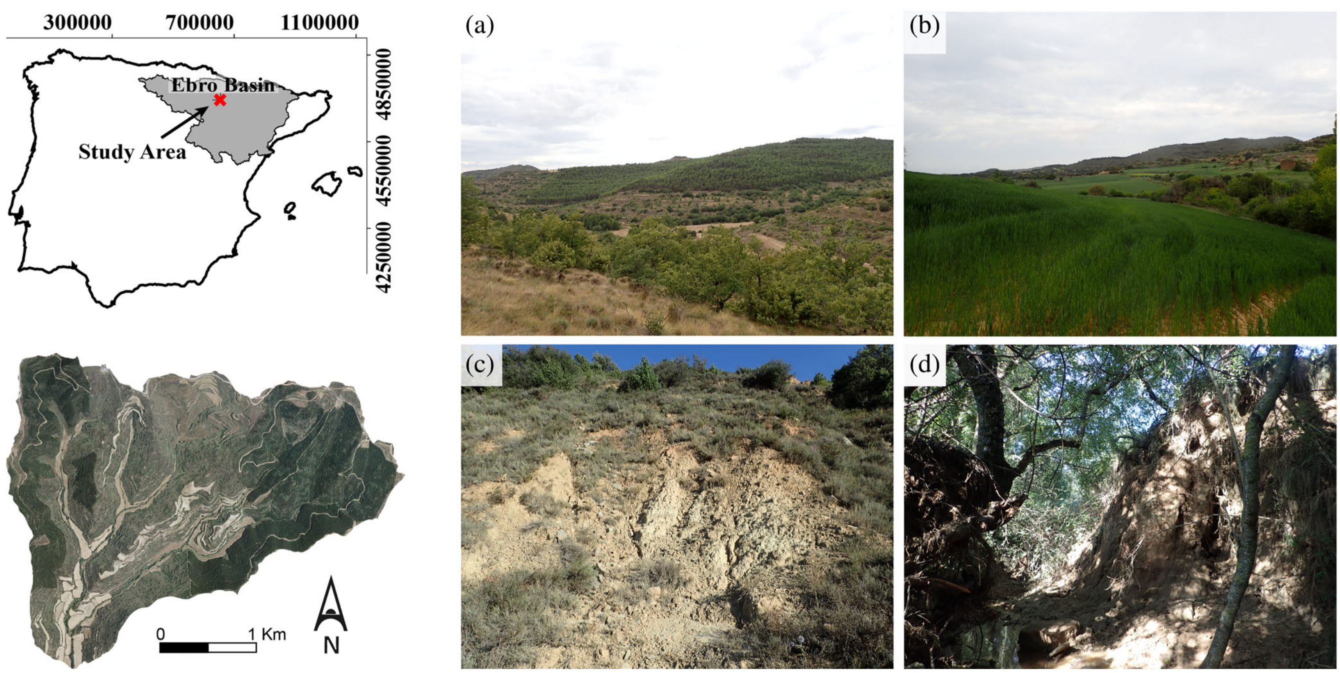

FIGURE 1 Location of the study area and photographs of the main land uses in the Cenera catchment (a, pine afforestation and open forest and scrubland in the front; b, croplands; c, barren land; d, stream banks in the incised stream. [Colour figure can be viewed at wileyonlinelibrary.com]

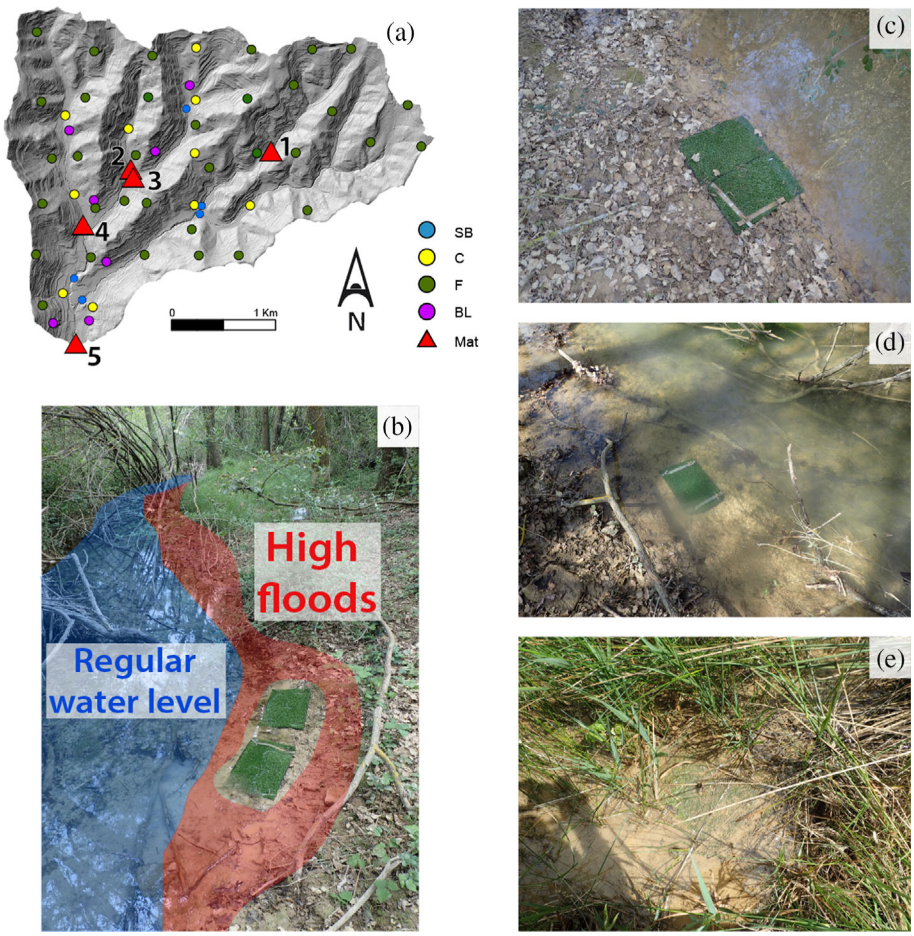

FIGURE 2 (a) Location of the soil sampling points in the Cenera catchment under different land uses/land covers (C, cropland; F, forest; BL, barren land; SB, streambanks) and of the trap MATs (Mat 1 to 5) for collecting sediment. b: Scheme of the study setup: The MATs are placed to retain the transported sediment below the water level reached during storm events triggering high floods (coloured in red). The regular water level is coloured in blue. (c–e) Photographs of the MATs during different events. (c) MAT5 after a flooding episode in campaign 18. (d) MAT 5 during a high water episode of a low energy event. (e) MAT4 full of sediment after a high-intensity rainfall and flood event collected in campaign 15. [Colour figure can be viewed at wileyonlinelibrary.com]

≤ 0.063 mm and the same parameters than in the sediment sources were evaluated in each sample.

2.4 | Rainfall characteristics

The characteristics of the rainfall events registered during each seasonal campaign were evaluated using the data recorded in a tipping bucket rain gauge located in the catchment, with information recorded at 1-min interval. The accumulated precipitation along the time period and in each erosive event (≥ 12 mm) (Xie et al., 2002), besides the maximum precipitation records in different intervals (24 h and 1 h) were considered in the analysis. The data was checked and completed when necessary with the information from Sos del Rey Católico (Lat: 42°29′ 50″N; Long: 1° 12′ 55″ O; elev: 639 m a.s.l. and Yesa (Lat: 42° 37′ 13″ N: Long: 1° 12′ 13″ O; elev: 490 m) meteorological stations, which belong to the Spanish Meteorological Agency-AEMET).

2.5 | Data analysis

The characteristics of the sediment sources in the catchment and their variability were assessed by taking surface samples (0–2 cm) under each land use/land (cover cropland, forest, scrubland, afforestation, streambank and barren land). The characteristics of the sediments collected in each period were analyzed and compared to the properties of the sediment sources in the upstream areas from which each MAT could receive eroded material. The relationships between different properties in the sources and in the sediments were evaluated using a multivariate analysis (correlation matrix). The differences in the composition of the sediments between campaigns were explained taking into account the characteristics of the recorded events. A cluster analysis was applied to the sediment properties, using the rainfall characteristics as external variables. The Ward (hierarchical) and the k-means methods were applied and the Euclidean distance was used to measure the similarity between the objects. The number of clusters was determined using the Elbow method calculating the total within-cluster sum of square for different number of clusters. In addition, the use of both methods allowed confirming the optimal number of groups. For the retained clusters, the centroids (average sediment characteristics) were evaluated as well as the characteristics of the rainfalls recorded in each period.

3 | RESULTS

3.1 | Soil properties under the different land uses

The average soil characteristics under the main land uses/land covers (sources) are shown in Table 1. The soils have high silt$_{sources}$ contents

TABLE 1 Average values and standard deviation of the properties in the surface layer (0–2 cm) of the sources: soil particle distribution-USDA, low frequency magnetic susceptibility ($\chi LF_{sources}$), soil organic matter ($SOM_{sources}$), total phosphorus ($P_{sources}$) and titanium ($Ti_{sources}$) concentration.

	$Clay_{sources}$ (%)	$Silt_{sources}$ (%)	$Sand_{sources}$ (%)	$\chi LF_{sources}$ (10^{-8} m^3/kg)	$P_{sources}$ (mg/kg)	$Ti_{sources}$ (mg/kg)	$SOM_{sources}$ (%)
Cropland	13.3 ± 2.9 a	70.9 ± 2.9 a	15.7 ± 3.1 ab	37.6 ± 18.4 ab	381 ± 83a	2972 ± 393 a	2.8 ± 1.4 a
Forest	14.5 ± 2.0 ab	70.9 ± 3.2 a	16.4 ± 2.5 ab	43.0 ± 21.8 a	267 ± 74 b	2999 ± 474 ab	7.8 ± 3.3 b
Scrubland	13.7 ± 4.6 ab	69.2 ± 4.7a	17.1 ± 4.2 ab	36.5 ± 30.0a	258 ± 117 b	2952 ± 497ab	8.0 ± 4.9 b
Afforest.	16.3 ± 4.9 a	69.0 ± 5.9 a	14.7 ± 5.8 ab	42.9 ± 21.4 ab	266 ± 33 b	3164 ± 489 a	5.0 ± 2.7 c
Streambank	13.8 ± 2.5 ab	73.3 ± 4.3 ab	12.9 ± 5.8 b	26.4 ± 15.1 b	291 ± 35 b	3318 ± 310 b	2.3 ± 0.7 ad
Barren land	11.2 ± 4.0 ab	74.7 ± 5.6 b	11.7 ± 8.3 b	12.2 ± 5.2 c	278 ± 23 b	2959 ± 272 a	0.5 ± 0.4 d

Note: Different letters indicate significant differences between land use/land cover.

TABLE 2a Correlation matrix of properties (USDA texture: $clay_{sources}$, $silt_{sources}$, $sand_{sources}$, soil organic matter ($SOM_{sources}$), low frequency magnetic susceptibility ($\chi LF_{sources}$) and total phosphorus ($P_{sources}$), titanium ($Ti_{sources}$) concentration) sampled at different locations within the catchment, considering all land uses/land covers together.

	$Clay_{sources}$	$Silt_{sources}$	$Sand_{sources}$	$\chi LF_{sources}$	$P_{sources}$	$Ti_{sources}$	$SOM_{sources}$
$Clay_{sources}$		−0.3248 ***	−0.3509 ***	0.3224 ***	0.2673 **	0.4955 ***	0.3459 ***
$Silt_{sources}$			−0.7716 ***	−0.6081 ***	−0.1046 NS	−0.3754 ***	−0.5042 ***
$Sand_{sources}$				0.3850 ***	−0.0175 NS	0.0381 NS	0.2664 **
$\chi LF_{sources}$					0.0961 NS	0.4971 ***	0.5482 ***
$P_{sources}$						0.2686 **	−0.0270 NS
$Ti_{sources}$							0.1703 NS

Abbreviation: NS, not significant.
Note: $p < 0.01$: significant at 99%; $p < 0.05$: significant at 95%; $p < 0.1$: significant at 90%.

(about 70%) and relatively low $clay_{sources}$ and $sand_{sources}$ contents (about 15%, on average). The $\chi LF_{sources}$ and the $SOM_{sources}$ presented significant differences among soils under the different land uses, with the highest values under forest and the lowest in the barren land. Regarding the rest of the properties, it was observed that the highest $P_{sources}$ values were recorded in croplands, followed by the streambanks. The higher $Ti_{sources}$ concentration, however, did not vary significantly between land uses/land covers, although the highest values were observed in the streambanks.

The relationships between the properties in the sources are presented in Table 2a and 2b. It can be seen that, when all land uses/land covers were analyzed together (Table 2a) $P_{sources}$ and $Ti_{sources}$ concentrations were positively correlated with $clay_{sources}$ content and with the $\chi LF_{sources}$ values. A positive relationship between $Ti_{sources}$ and $\chi LF_{sources}$ and between $P_{sources}$ and $Ti_{sources}$ was also confirmed. $\chi LF_{sources}$ correlated positively with $SOM_{sources}$. However, no significant relationship was found between $SOM_{sources}$ and $P_{sources}$ or $Ti_{sources}$. Considering the analysis separately by land use/land cover, most of these relationships disappeared in the soils under croplands, in the barren land and in the streambanks, but remained in the soils under forest land uses (forest, afforested areas and scrublands) and in addition, a positive relationship between $P_{sources}$ and $SOM_{sources}$ was confirmed under forest land uses and in the streambanks (Table 2b).

3.2 | Rainfall characteristics

The erosive rainfall events ($R > 12$ mm) recorded during the 20 monitoring campaigns are summarized in Table 3. The accumulated precipitation in the erosive events for each period ranged between about 59.4 and 318.3 mm. The number of events included in each campaign varied between two and eight, and in 80% of the campaigns at least one event accumulated more than 40 mm of rainfall. The precipitation for each individual event ranged between 13 and 95.6 mm. Some events lasted more than 24 h, and the maximum P_{24h} reached values of up to 77.0 mm. In addition, some events recorded high precipitation concentration in a short time period, with hourly intensities of up to 50.4 mm/h. Besides the erosive events, other rainfall events that

TABLE 2b Correlation matrix of properties (USDA texture: $clay_{sources}$, $silts_{ources}$, $sand_{sources}$, soil organic matter ($SOM_{sources}$), low frequency magnetic susceptibility ($\chi LF_{sources}$) and total phosphorus ($P_{sources}$), titanium ($Ti_{sources}$) concentration) sampled at different locations within the catchment, under different land uses/land covers: cropland (C), forest (F), streambanks (SB) and barren land (BL).

Cropland (C)								Forest + afforested + scrub (F)							
	$Clay_C$	$Silt_C$	$Sand_C$	χ_{LFC}	P_C	Ti_C	SOMc		$clay_F$	$silt_F$	$sand_F$	$\chi_{LF\ F}$	P_F	Ti_F	SOM_F
$Clay_C$		−0.119	−0.393	0.209	0.720	0.510	0.346	$Clay_F$		−0.518	−0.348	0.388	0.565	0.687	0.386
		NS	NS	NS	**	NS	NS			***	**	**	***	***	**
$Silt_C$			−0.866	−0.318	0.256	−0.144	−0.354	$Silt_F$			−0.621	−0.645	−0.401	−0.565	−0.425
			***	NS	NS	NS	NS				***	***	**	***	***
$Sand_C$				0.189	−0.600	−0.123	0.125	$Sand_F$				0.351	−0.078	−0.010	0.109
				NS	NS	NS	NS					**	NS	NS	NS
χLF_C					0.311	0.492	0.451	χLF_F					0.269	0.656	0.398
						NS	NS						NS	***	**
P_C						0.306	0.080	P_F						0.640	0.470
						NS	NS							***	***
Ti_C							0.492	Ti_F							0.288
							NS								NS

Streambank (SB)								Barren land (BL)							
	$Clay_{SB}$	$Silt_{SB}$	$Sand_{SB}$	χLF_{SB}	P_{SB}	Ti_{SB}	SOM_{SB}		$Clay_{BL}$	$Silt_{BL}$	$Sand_{BL}$	$\chi_{LF\ BL}$	P_{BL}	Ti_{BL}	SOM_{BL}
$Clay_{SB}$		0.258	−0.642	0.210	0.239	−0.125	0.275	$clay_{BL}$		0.232	−0.448	−0.434	0.074	0.641	−0.365
		NS	**	NS	NS	NS	NS			NS	NS	NS	NS	NS	NS
$Silt_{SB}$			−0.906	−0.602	−0.203	−0.730	−0.067	$silt_{BL}$			−0.974	0.096	−0.601	−0.279	−0.130
			***	**	NS	***	NS				***	NS	NS	NS	SN
$Sand_{SB}$				0.386	0.057	0.634	−0.068	$sand_{BL}$				0.008	0.538	0.104	0.293
				NS	NS	**	NS					NS	NS	NS	NS
χLF_{SB}					0.432	0.427	0.576	χLF_{BL}					−0.534	−0.028	0.325
					NS	NS	**						NS	NS	NS
P_{SB}						0.333	0.666	P_{BL}						0.048	0.167
						NS	***							NS	NS
Ti_{SB}							0.071	Ti_{BL}							0.148
							NS								NS

Abbreviation: NS, not significant.
Note: ***Significant at 99%. **Significant at 95%. *Significant at 90%.

TABLE 3 Summary of the rainfall events recorded in each analyzed monitoring campaign and their characteristics (accumulated precipitation in erosive and in non-erosive events (R_t), maximum precipitation recorded in one event (REmax), maximum precipitation recorded in 24 h ($Rmax_{24h}$) and maximum hourly intensity ($I_h$max).

Camp.	Sampling date	P_{total} (erosive + non-erosive)(mm)	Number of erosive events	REmax (mm)	$Rmax_{24h}$ (mm)	$I_h$max (mm/h)
1	28-10-2014	318.3 + 6.9	6	101.0	67.8	29.4
2	15-4-2015	285.7 + 37.4	8	63.2	27.4	15.2
3	7-7-2015	95.6 + 8.5	3	46.1	25.6	7.0
4	22-9-2015	80.4 + 9.3	5	21.2	21.2	15.7
5	21-12-2015	113.3 + 7.5	4	49.6	32	7.2
6	22-3-2016	198.7 + 11.5	7	42.5	20.9	5.3
7	17-6-2016	63 + 22.6	3	32.8	15.2	8.4
8	22-9-2016	59.4 + 10.4	2	43.8	24.2	13
9	21-12-2016	143.8 + 31.0	3	75.8	57.6	6.4
10	31-3-2017	141.8 + 17.6	4	51.0	35.2	9.6
11	27/06/2017	130.2 + 48.2	5	47.0	42.8	21.8
12	22/09/2017	84.2 + 23.2	2	62.6	53.6	11.8
13	26/12/2017	68.6 + 7.3	2	46.2	45.6	9.8
14	6/4/2018	148.0 + 30.8	5	50.6	16.8	5.2
15	28/06/2018	223.8 + 11.9	4	95.6	38.8	19.5
16	20/09/2018	144.2 + 4	4	73.6	73.6	50.4
17	21/12/2018	142.8 + 20.8	5	40.5	40.5	8.2
18	18/03/2019	98.5 + 7.8	2	71.2	16.4	2.8
19	20/06/2019	161.0 + 33.8	5	83.0	77.0	16.8
20	18/10/2019	89.4+ 13.6	3	46.1	29.6	19.6

accumulated small amounts were also recorded, contributing to an increase in soil moisture (the amount of rainfall of the non-erosive events is also indicated in Table 3).

3.3 | Characteristics of sediments collected at the outlet of the Cenera catchment

High variability in clay and sand contents was observed among sediments (sed) collected at the catchment outlet (MAT5) in the different monitoring campaigns (Figure 3). In most of them, $clay_{sed}$ content was smaller than in the sources under the main land uses. Only in four campaigns, $clay_{sed}$ content (ranging between 4.7 and 21.7%) was higher than $clay_{sources}$. An opposite result was obtained regarding the $sand_{sed}$ content, which ranged between 7.5 and 35.5%. However, for all campaigns the differences in $silt_{sed}$ content were very small (average values 69.4%) and similar to the existing in the sources. The SOM_{sed} content presented high variability among periods, with an average value of 2.91% (ranging between 0.75 and 5.32%), which mean values of the same order of magnitude of the recorded in the croplands and streambanks, but much lower than the $SOM_{sources}$ in the forest land uses. The χLF_{sed} had much lower values in the sediments than in the original sources except in the barren land. Regarding the chemical composition of the sediments, there were clear differences in P_{sed} between the analyzed campaigns, with P_{sed} > $P_{sources}$ under most of the land uses/land covers. In almost 50% of the analyzed campaigns, P_{sed} were higher than the $P_{sources}$ levels existing in croplands. There was a significant positive linear correlation between P_{sed} concentration and SOM_{sed} ($r^2 = 0.88$), between P_{sed} and $clay_{sed}$ content ($r^2 = 0.52$) and between P_{sed} and the χLF_{sed} values ($r^2 = 0.63$). All relationships are shown in Table 4 (data corresponding to MAT 1–MAT 5).

3.4 | Relationships between sediment and rainfall characteristics

The results of the cluster analysis, based on particle size, SOM_{sed} content and the χLF_{sed} values, gave rise to similar classification applying both cluster methods (Ward and k-means). The analyzed campaigns were classified into three clusters according to the Ward method and four clusters according to k-means. The difference consisted of one observation (campaign 8) that was separated in one cluster in the k-mean analysis, while in the Ward analysis they formed a subgroup in cluster C2 (although at higher distance than the rest of observations) (Figure 4). Cluster C1 and C2 grouped 35% of the campaigns, each, while cluster C3 grouped 30% of the total.

The centroids of the clusters are shown in Table 5. Cluster C1 grouped the events which lead to lower $clay_{sed}$ and high $sand_{sed}$ contents and the lowest SOM_{sed}, χLF_{sed} and P_{sed} concentration. Cluster

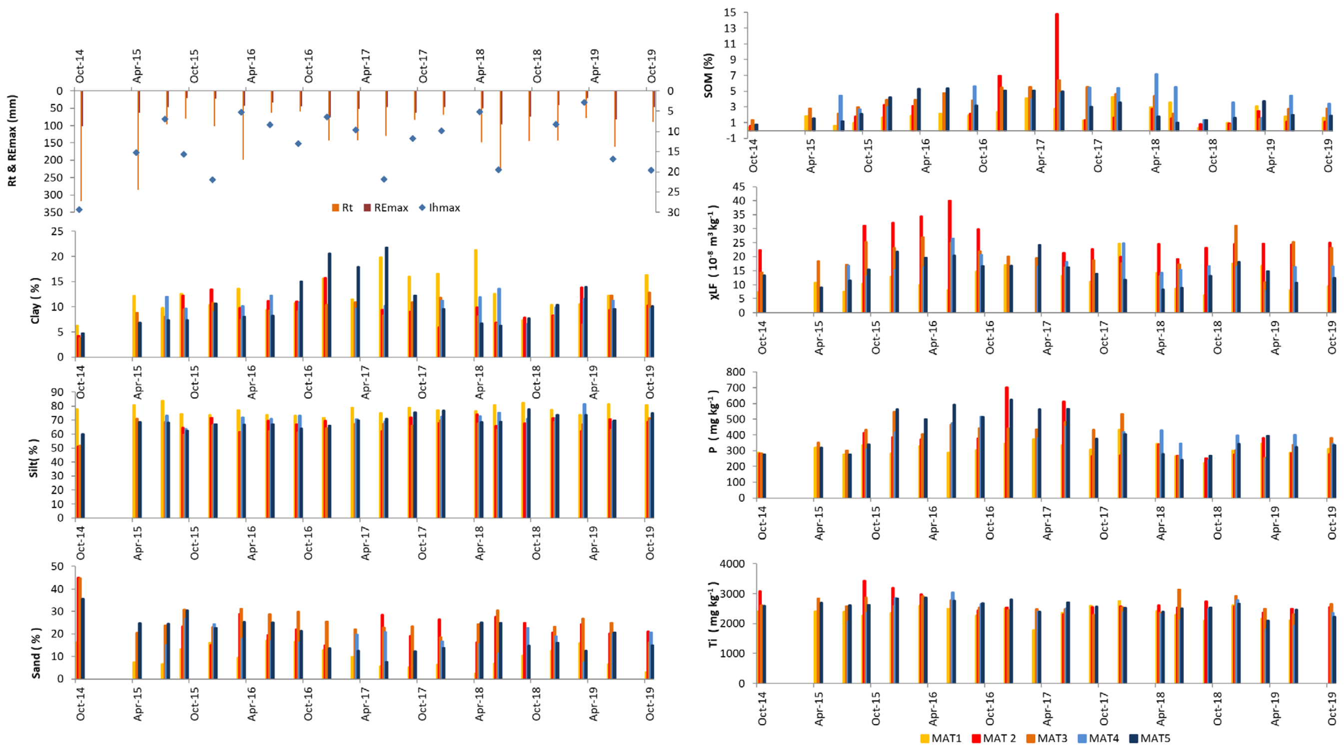

FIGURE 3 Precipitation characteristics (total accumulated precipitation (Rt), maximum precipitation in one event (REmax) and maximum hourly rainfall intensity ($I_h$max)) and properties (USDA texture: $clay_{sed}$, $silt_{sed}$, $sand_{sed}$, SOM_{sed}, low frequency magnetic susceptibility (χLF_{sed}) and total phosphorus (P_{sed}) and titanium (Ti_{sed}) concentrations of the sediments collected at the five locations within the catchment along the analyzed campaigns. [Colour figure can be viewed at wileyonlinelibrary.com]

C2 grouped the campaigns in which the sediments had the highest $clay_{sed}$ and SOM_{sed} contents and also the highest χLF_{sed} and P_{sed} concentrations, which was near double than that of cluster C1. Cluster C3 grouped the campaigns that gave rise to sediments with intermediate characteristics regarding to $clay_{sed}$, SOM_{sed} and χL_{sed} but were richer in $silt_{sed}$ content. In C3, P_{sed} concentration also had intermediate values, while the events grouped in C3 cluster had the highest Ti_{sed} concentration. The isolated episodes in C4 (k-means method), (equivalent to sub-cluster C2.2, Table 5) had similar values to the average of cluster C2, except for SOM and χLF_{sed}, which were slightly smaller.

Looking at the characteristics of the rainfalls for the periods included in each group, it could be observed that C1 included the periods that accumulated the highest total precipitation and with high precipitation in individual events. In C1, all campaigns were recorded in spring and most of events were of long duration (several days). The number of events was higher than in the rest of the periods (up to eight events, with five events on average). The average total precipitation was 182.8 mm, with up to 318.3 mm in erosive events and up to 323.1 mm considering the rainfall accumulated in non-erosive events. The average event precipitation was 39 mm with up to 101 mm, and with the maximum precipitation in 24 h of up to 77 mm. Clusters C2 and C3 grouped seasonal campaigns with similar average number of rainfall events (three or four erosive events in the period), but they had different characteristics. In all cases, the events had lower total precipitation than those recorded in the events of cluster C1. The campaigns in clusters C2 and C3 recorded less precipitation than those in cluster C1, but with higher precipitation concentration (up to 75.8 and 73.6 mm per event, and of up to 52.6 mm and 73.6 mm in 24 h in C2 and C3, respectively). In addition, the precipitation accumulated in smaller periods was higher in the events grouped in C3 than in C2, (maximum hourly intensity $I_h = 50.4$ mm/h in C3 vs. 21.9 mm/h in C2). Though events grouped in C2 were recorded in all seasons over the years, the high intensity events included in cluster C3 were recorded in autumn (50% of the periods). The campaign isolated in the sub-cluster C2.2 (cluster C4 in k-means) recorded fewer events and less total precipitation than the average of cluster C2, but it included at least one high magnitude event.

3.5 | Variability in the sediment composition recorded across the catchment

The average characteristics of the sediments, recorded during the 20 monitoring campaigns at the different catchment locations, are shown in Table 6. The sediments were rich in $silt_{sed}$ in all locations (> 65%) and there was not a clear trend in the $clay_{sed}$ and $sand_{sed}$ contents between the sampling locations up and downstream. However, despite the variability among periods, the lowest SOM_{sed} and P_{sed} contents were observed in the MATs located at the headwaters (MAT1 and MAT2) and their values increased within the stream from up to down (MAT1 → MAT3, and MAT2 → MAT4) (Figure 3). At the catchment outlet, however, while the average P_{sed} presented

TABLE 4 Correlation matrix of the sediment properties collected at the five locations of the MATs within the catchment (MAT1–MAT5).

	MAT1						MAT2						MAT3					
	$Silt_{sed}$	$Sand_{sed}$	χLF_{sed}	P_{sed}	Ti_{sed}	SOM_{sed}	$Silt_{sed}$	$Sand_{sed}$	χLF_{sed}	P_{sed}	Ti_{sed}	SOM_{sed}	$Silt_{sed}$	$Sand_{sed}$	χLF_{sed}	P_{sed}	Ti_{sed}	SOM_{sed}
$Clay_{sed}$	−0.206	−0.683	0.347	0.552	0.206	0.373	0.390	−0.719	0.657	0.685	−0.068	−0.147	0.517	−0.746	0.384	0.584	−0.356	0.449
	NS	***	*	**	NS	NS	NS	***	***	***	NS	NS	**	***	NS	***	NS	NS
$Silt_{sed}$			−0.421	−0.378	−0.159	−0.168		−0.920	0.175	9E-04	−0.326	0.134		−0.953	−0.034	0.139	−0.117	0.171
			**	NS	NS	NS		***	NS	NS	NS	NS		***	NS	NS	NS	NS
$Sand_{sed}$			0.023	−0.180	−0.053	−0.187			−0.391	−0.292	0.276	−0.055			−0.099	−0.331	0.226	−0.319
			NS	NS	NS	NS			*	NS	NS	NS			NS	NS	NS	NS
χLF_{sed}				0.828	0.483	0.561				0.372	0.373	−0.096				0.266	0.394	−0.081
				***	**	***				NS	NS	NS				NS	*	NS
P_{sed}					−0.198	0.631					−0.146	0.219					−0.219	0.759
					NS	***					NS	NS					NS	***
Ti_{sed}						−0.026						−0.257						−0.446
						NS						NS						**

	MAT4						MAT5					
	$Silt_{sed}$	$Sand_{sed}$	χLF_{sed}	P_{sed}	Ti_{sed}	SOM_{sed}	$Silt_{sed}$	$Sand_{sed}$	χLF_{sed}	P_{sed}	Ti_{sed}	SOM_{sed}
$Clay_{sed}$	0.498	−0.733	0.068	0.355	−0.259	0.647	0.121	−0.748	0.469	0.720	0.038	0.662
	**	***	NS	NS	NS	***	NS	***	**	***	NS	***
$Silt_{sed}$		−0.955	−0.219	−0.189	−0.335	0.069		−0.749	−0.180	−0.186	−0.445	−0.038
		***	NS	NS	NS	NS		***	NS	NS	**	NS
$Sand_{sed}$			0.148	0.035	0.355	−0.265			−0.192	−0.356	0.272	−0.416
			NS	NS	NS	NS			NS	NS	NS	*
χLF_{sed}				0.642	0.551	0.474				0.792	0.361	0.739
				***	**	NS				***	NS	***
P_{sed}					0.520	0.760					0.448	0.938
					**	***					**	***
Ti_{sed}						0.051						0.317
						NS						NS

Abbreviation: NS, not significant.
Note: ***Significant at 99%. **Significant at 95%. *Significant at 90%.

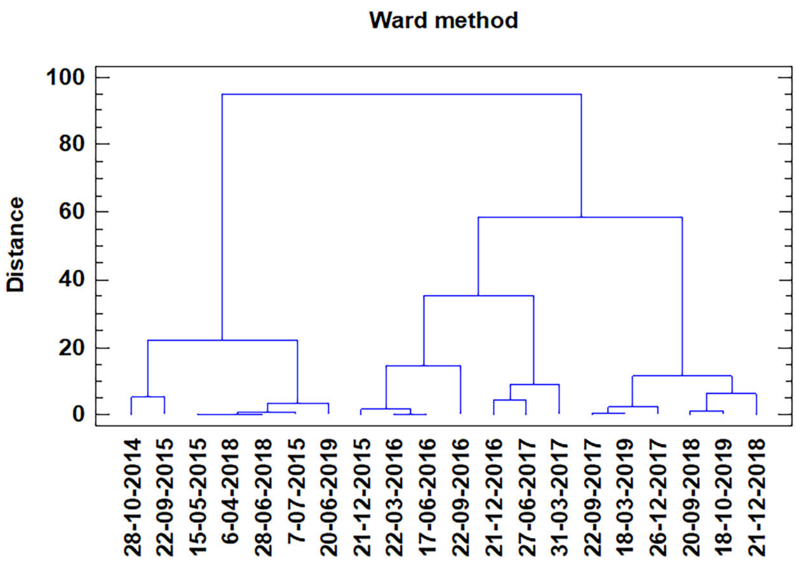

Monitoring campaign	Collecting data	Cluster method	
		Ward	k-means
1	28/10/2014	1	1
2	15/04/2015	1	1
3	7/07/2015	1	1
4	22/08/2015	1	1
5	21/12/2015	2	2
6	22/03/2016	2	2
7	17/07/2016	2	2
8	22/09/2016	2	4
9	21/12/2016	2	2
10	31/03/2017	2	2
11	27/06/2017	2	2
12	22/09/2017	3	3
13	26/12/2017	3	3
14	6/04/2018	1	1
15	28/06/2018	1	1
16	20/09/2018	3	3
17	21/12/2018	3	3
18	18/03/2019	3	3
19	20/06/2019	1	1
20	18/10/2019	3	3

FIGURE 4 Monitoring campaign classification using Ward's and k-means hierarchical clustering method, based on the sediment composition obtained at the catchment outlet. [Colour figure can be viewed at wileyonlinelibrary.com]

TABLE 5 Centroids of the cluster analysis based on the sediment composition at the catchment outlet.

	$Clay_{sed}$ (%)	$Silt_{sed}$ (%)	$Sand_{sed}$ (%)	χLF_{sed} (10^{-8} m^3/kg)	P_{sed} (mg/kg)	Ti_{sed} (mg/kg)	SOM_{sed} (%)
C1	6.9	66.5	26.5	11.0	293	2532	1.47
C2	14.6	66.6	19.7	18.9	531	2632	4.39
C2.1	14.5	67.8	17.7	19.8	567	2433	4.98
C2.2 (C4 in k-means)	15.0	63.7	21.3	16.6	514	2680	3.20
C3	10.6	75.4	14.0	14.0	353	2787	2.50

TABLE 6 Average (± SD) of the sediment characteristics recorded at the different locations within the catchment (soil particle distribution (USDA), low frequency magnetic susceptibility (χLF_{sed}), total phosphorus concentration (P_{sed}), titanium (Ti_{sed}) and soil organic matter (SOM_{sed}).

	$Clay_{sed}$ (%)	$Silt_{sed}$ (%)	$Sand_{sed}$ (%)	χLF_{sed} (10^{-8} m^3/kg)	P_{sed} (mg/kg)	Ti_{sed} (mg/kg)	SOM_{sed} (%)
MAT1	12.5 ± 4.9	77.5 ± 3.5	10.0 ± 6.2	12.4 ± 5.2	312 ± 88	2362 ± 230	2.0 ± 1.7
MAT2	9.7 ± 2.9	66.5 ± 5.5	23.9 ± 7.2	26.7 ± 5.8	353 ± 127	2721 ± 349	2.8 ± 3.5
MAT3	9.1 ± 2.2	65.0 ± 4.7	25.7 ± 6.2	20.2 ± 5.1	389 ± 88	2622 ± 230	3.5 ± 1.7
MAT4	10.7 ± 1.6	71.4 ± 3.7	17.9 ± 4.7	16.8 ± 4.2	383 ± 75	2365 ± 367	4.1 ± 1.6
MAT5	11.0 ± 4.7	69.9 ± 4.4	19.0 ± 6.3	15.0 ± 4.5	410 ± 125	2574 ± 203	3.0 ± 1.6

the highest values, the SOM_{sed} and the χLF_{sed} were smaller than in the intermediate positions. Regarding χLF_{sed}, the highest average values were recorded in MAT2 and MAT3 and the lowest in MAT1 and MAT5.

Given the differences observed between sampling locations, a detailed analysis was done point by point. The correlation matrix for each location is shown in Table 4. The positive relationships found at the catchment outlet between P_{sed} and $clay_{sed}$ and between P_{sed} and SOM_{sed} were confirmed at four of the five locations (MATs 1, 2, 3, and 5 for clay and MATs 1, 3, 4, and 5 for SOM), while positive correlations between P_{sed} and χLF_{sed} were observed at three of the five locations (MATS 1, 4, and 5). P_{sed} was also positively correlated with Ti_{sed} in MATs 4 and 5.

4 | DISCUSSION

4.1 | Relationship between phosphorus loss and rainfall features

The high silt content in the sources of the Cenera catchment (about 70% under all land uses/land covers- Table 1) made them very susceptible to suffer erosion processes. A similar proportion of silt was maintained in the sediments, which was the predominant fraction, with very little variability among campaigns. However, some differences were observed in the $clay_{sed}$ and $sand_{sed}$ contents (Figure 3), which differ in some cases from the contents in the sources. The highest $clay_{sed}$ contents occurred in the campaigns with higher precipitation concentration (C2), that is, under high-intensity rainfall events that accumulate greater energy in shorter periods of time. The rainfall energy in those events is strong enough to detach the clay particles that are usually bound by greater cohesive forces.

The enrichment of sediment in clay size particles could be explained by a first enrichment process due to particle entrainment and to a further re-deposition of coarser particles (Novotny & Chesters, 1989). The result observed in the sediment composition in our catchment is in agreement with the changes recorded in the composition of the sediments deposited in channel beds of the main catchment to which the Cenera stream is a tributary after an exceptional rainfall event (Ramos et al., 2022), which led to a decrease in the proportion of clay and an increase in the proportion of sand. The average values of $clay_{sed}$ were near double in the sediments recorded in the events grouped in clusters C2 and C3, which happened in the periods with higher rainfall intensity, than in those grouped in cluster C1 (Table 5), which were recorded in the periods with high total precipitation but of lower intensities. The positive correlations between P_{sed} and $clay_{sed}$ and SOM_{sed}, and the enrichment in P in the sediments compared to that in the soil confirm that the mobilization of the material contributes to mobilize also the P linked to fine soil particles.

Udawatta et al. (2004) found that the highest soil P loss occurred in years with above normal precipitation while Zimmer et al. (2016) and Sharpley et al. (2008) point out the importance of storm events for P release from the catchments and its transfer to water bodies. However, within the storm characteristics, rainfall concentration and intensity play a particular role (Fraser et al., 1999; Shigaki et al., 2007). The effect of rainfall intensity on the mobilization of P has been documented by different authors (Joel et al., 2012; Kuhn et al., 2012; Messing et al., 2015; Wang et al., 2022). For the main land uses in the study catchment, the direct effect of increasing rainfall intensity in soil and P losses was verified under simulated rainfall in laboratory conditions (Ramos et al., 2019), and the results obtained under natural rainfall along the period analyzed corroborate their effect on the P mobilization. Thus, higher particulate P transport is likely associated with increasing peak discharge that increases with rainfall intensity, as indicated by Quinton et al. (2001), who suggest that greater flow energies associated with higher discharge rates may remove more P-rich material.

The effect of the magnitude of the events on P mobilization is also confirmed when the events included in clusters C2 and C3 are compared. While the events in both clusters accounted for similar total accumulated rainfall, the periods in which the events accumulated less water per event led to lower P_{sed} concentration, while the highest P_{sed} concentrations were recorded under higher intensity events (C2), which occurred mainly in autumn. These high intensity events, led to the sediments with higher $clay_{sed}$ and P_{sed} concentrations. This result agrees with the loss of clay and P in the streambeds observed after an exceptional rainfall event analyzed in the area that exported the finest sediments and associated P out of the main catchment (Ramos et al., 2022).

4.2 | Spatial variability of the P concentration in the sediments and its relation to source properties and land use

The P concentration was much lower in MAT1 than in MAT5, which could seem contradictory to that mentioned before regarding the relationship between P_{sed} and $clay_{sed}$ found at the outlet. However, it may be justified according to the main land uses existing upstream of each MAT. Different authors have pointed to croplands as the main contributing source to total P and its higher contribution compared to other land uses has been documented in several studies (Ulén & Kalisky, 2005; Otero et al., 2011; Neidhardt et al., 2019; Räty et al., 2020; Tian et al., 2022). In our study case, MAT1 receives water from areas where the predominant land uses are forest and scrubs in which $P_{sources}$ levels are smaller than under croplands, while MAT5 receives water from areas that have all land uses, including croplands, which have the highest $P_{sources}$ values.

The higher proportion of croplands close to the catchment outlet could justify the higher P mobilization in the area around the outlet, which agrees with the results found by Ghafari et al. (2017) who identified high hazard areas in agricultural lands and in sub-basins located close to a watershed outlet where the sediment and phosphorus yield were higher. In this respect, Neidhardt et al. (2019) found total P levels in soil and sediment at farmland sites more than twofold higher than in forestry sites, and Räty et al. (2020) recorded total P losses about 30 times higher in agricultural than in forestry subcatchments. In addition, McDowell et al. (2001) indicate that P concentrations are controlled by overland flow and that erosion from areas of the catchment coincident with high soil P can be also influenced by the channel sediments. Gburek and Sharpley (1998) also indicate that runoff production zones are the areas that control most of the P transport. As mentioned by Steegen et al. (2000), additional geomorphological features affect sediment delivery and export out of a catchment. However, P losses can differ among management practices (Dugan et al., 2022; Fang, 2021; Ramos et al., 2015; Wang et al., 2017).

The analysis of the soil properties showed that P was linked to the finest fraction as indicated by the relationships between $P_{sources}$ and $clay_{sources}$ considering all land uses (Table 2a). This result was also confirmed for the main land uses (cropland and forest land, Table 2b). Accordingly, the events that gave rise to sediments with higher $clay_{sed}$ content also led to higher P_{sed} concentrations, which means higher P exportation.

Nevertheless, the P_{sed} differed among sampling locations, although the relationship between $P_{\mathbf{sed}}$ and $clay_{sed}$ was maintained, and apart from MAT4 was significant in all the MATs. The differences in these relationships could be due to the disturbance processes that take place under different land uses. Clay content is an important binding agent of P and influences the particulate P losses (Djodjic et al., 2021). In our study case, the results recorded after the events of different characteristics confirmed the binding between P and clay, and that the mobilization of the clay fraction under high intensity rainfall leads to the mobilization of significant amounts of P. The lack of significance in MAT4 could be due to the higher contribution of barren land and streambanks to that MAT, which has lower $P_{sources}$ concentration and for which the clay-P relationship was not significant (Table 2b). In addition, the P concentration was also correlated with the SOM content in the sediments and in the soils under forest. SOM has been identified as an important factor affecting the adsorption–desorption of soil P (Yang et al., 2019).

The sediments richest in P_{sed} were the ones that had the highest SOM_{sed}. Within the Cenera catchment, P_{sed} and SOM_{sed} had higher average values in the areas where forest land use (forest, scrub and afforested areas) is predominant corresponding to the locations of MATs 1 to 4, compared to the area where croplands cover higher surface (MAT5). However, there was an increase in both SOM_{sed} and P_{sed} along the streams (MAT1 → MAT3, MAT2 → MAT4), which could be due to the effect of the increasing runoff downstream. Furthermore, the highest P_{sed} and SOM_{sed} values were recorded for the events with higher precipitation accumulation (C2, Table 5). Deng et al. (2021) found P loads in surface runoff, mainly driven by particulate P, also positively correlated with total carbon loads.

Additional information on P changes caused by erosion could be extracted from the χLF values. The highest χLF values existed in the soils under forest, followed by the rest of the predominant land uses (scrub, afforestation, and cropland), which was higher than in the barren land and streambanks. The $\chi LF_{sources}$ was positively correlated with $clay_{sources}$ (Table 2a), which agrees with the results found by Barbosa et al. (2021), besides, this relationship is mainly driven by the one existing in the forest land use (Table 2b). The relationship between $\chi LF_{sources}$ and $clay_{sources}$ observed in the sources was maintained in the sediments at three of the five locations (MATs 1-3-5), and although, there was not significant relationship between $P_{sources}$ and $\chi LF_{sources}$, and despite the smaller values of χLF_{sed} compared to $\chi LF_{sources}$, a strong significant correlation was found between χLF_{sed} and P_{sed} at the catchment outlet (MAT5) and in other two MATs (MAT1 and 4). Furthermore, the significant correlations between χLF_{sed} and SOM_{sed} and in turn between χLF_{sed} and P_{sed} in MATs 1 and 5, could be indicative of the P accumulation. As P is mainly stored in the soil surface, the higher χLF values in the forest soils are consistent with the lower disturbance degree that they suffer. These results also agree with the decrease of χLF associated to the decrease with soil depth found by Sanjari et al. (2021) in sedimentary parent materials and as an indicator of soil loss of surface layers by erosion processes (Lima et al., 2020; Quijano et al., 2014). In the same direction, a decrease in χLF values has been found in streambed sediments after an exceptional rainfall event in the area (Ramos et al., 2022). Therefore, the lower χLF_{sed} compared to $\chi LF_{sources}$ likely indicates that the poorest and more degraded soils in the Cenera catchment contribute in higher proportion to the transported sediments.

On the other hand, the relationships between χLF and Ti values (Table 2), confirm that both properties give information in the same direction and that they could be useful for identifying changes in the soil surface. The low values of Ti in the trapped sediment could be due to the provenance from deeper soil layers that are likely linked to soil losses by erosion. The results found in this research indicate a relationship between Ti and χLF under forest land use where soils are better preserved and have lower erosion rates (Lizaga et al., 2019). However, the Ti and χLF relationships disappear in cropland and barren land (Table 2b), where according to Lizaga et al. (2019), soil degradation by erosion is higher. The lack of correlation between Ti and χLF in the streambanks is explained by their own origin, since they are sediments, not soils.

In the sediments collected along the monitoring campaigns at the different locations in the catchment, Ti_{sed} and χLF_{sed} had in common that their values were much lower in the sediments than in the sources. The relationships between χLF_{sed} and Ti_{sed} were significant in four of the five MATs, and there were also differences between locations. The differences in χLF are in agreement with the values found in the soils of the areas that contribute to each MAT except for MAT1. As previously mentioned, χLF values can reflect the intensity of processes occurring at different landscape positions pointing to differences between headwaters and downstream locations in terms of different land uses and the amount of runoff circulating in the streams after the rainfall events. This could justify the lower χLF values found in the sediments recorded at the catchment outlet in MAT5, where besides accumulating higher runoff the cropland proportion is greater than in the other intermediate MATs locations of the catchment.

5 | CONCLUSIONS

The information extracted from the 20 monitored campaigns confirmed the influence of rainfall intensity as well as the effect of the increasing flow along the streams until the catchment outlet in P mobilization and conveyance. The analysis of the characteristics of the sediment sources and sediments collected across the catchment has provided insights into how P is bound to soil particles. P-clay binding was confirmed in all sediment sources while P-SOM binding was found only under forest land use. An enrichment in P was observed in the sediments where both P-clay and P-SOM bindings were observed. The lower χLF values in the sediments than in the soils, likely denote that the more degraded soils are more prone to be detached and transported. In addition, the results confirmed the higher contribution of croplands to P losses compared to other land uses/land covers, which is due not only to a higher susceptibility of soil to be eroded because of its lower vegetation cover, but also due to their location in areas that experience higher water accumulation of runoff generated upstream.

The results suggest that, particularly in Mediterranean areas, where both precipitation concentration of high intensity events are expected to increase, P mobilization and its loss, in particular from croplands, may generate higher water pollution problems in the future. Therefore, it would be necessary to adopt appropriate management practices in these areas and other of similar environments to reduce soil and nutrient losses.

ACKNOWLEDGMENTS

This research is part of the Project I + D + i PID2019-104857RB-I00, funded by the MCIN/ AEI/10.13039/501100011033/. This research article received aid of a predoctoral contract BES-2015-071780 of the project CGL2014-52986-R. The contribution of Ivan Lizaga was supported by the Research Foundation-Flanders (FWO, mandate 12V8622N).

CONFLICT OF INTEREST STATEMENT

There is no conflict of interest.

DATA AVAILABILITY STATEMENT

Research data are not shared.

ORCID

María Concepción Ramos https://orcid.org/0000-0003-4874-9750

Ana Navas https://orcid.org/0000-0002-4724-7532

REFERENCES

Abbasnia, M., & Toros, H. (2018). Analysis of long-term changes in extreme climatic indices: A case study of the Mediterranean climate, Marmara region, Turkey. *Pure and Applied Geophysics*, *175*, 3861–3873. https://doi.org/10.1007/s00024-018-1888-8

Barbosa, J. Z., Poggere, G., Silva, S. H. G., Mancini, M., Motta, A. C. V., Marques, J. J. G. D. S. E. M., & Curi, N. (2021). National-scale spatial variations of soil magnetic susceptibility in Brazil. *Journal of South American Earth Sciences*, *108*, 103191. https://doi.org/10.1016/j.jsames.2021.103191

Da Silva, R. F., Santos, G. G., Nóbrega, J. C. A., De Oliveira, G. C., De Oliveira Dias, B., Santos, D. P., & Da Silva, J. P. (2017). Impacts of land-use and management systems on organic carbon and water-physical properties of a Latossolo Amarelo (Oxisol). *Semina Ciencias Agrarias*, *38*, 109. https://doi.org/10.5433/1679-0359.2017v38n1p109

Deng, L., Sun, T., Fei, K., Zhang, L., Fan, X., Wu, Y., Ni, L., & Sun, R. (2021). Coupling loss characteristics of N-P-C through runoff and sediment in the hilly region of SE China under simulated rainfall. *Environmental Science and Pollution Research*, *28*, 37204–37216. https://doi.org/10.1007/s11356-021-13186-0

Djodjic, F., Bieroza, M., & Bergström, L. (2021). Land use, geology and soil properties control nutrient concentrations in headwater streams. *Science of the Total Environment*, *772*, 145108. https://doi.org/10.1016/j.scitotenv.2021.145108

Dugan, I., Pereira, P., Barcelo, D., Telak, L. J., Filipovic, V., Filipovic, L., Kisic, I., & Bogunovic, I. (2022). Agriculture management and seasonal impact on soil properties, water, sediment and chemicals transport in a hazelnut orchard (Croatia). *Science of the Total Environment*, *839*, 156346. https://doi.org/10.1016/j.scitotenv.2022.156346

Fang, H. (2021). Effect of soil conservation measures and slope on runoff, soil, TN, and TP losses from cultivated lands in northern China. *Ecological Indicators*, *126*, 107677. https://doi.org/10.1016/j.ecolind.2021.107677

Fraser, A. I., Harrod, T. R., & Haygarth, P. M. (1999). The effect of rainfall intensity on soil erosion and particulate phosphorus transfer from arable soils. *Water Science and Technology*, *39*, 41–45. https://doi.org/10.1016/S0273-1223(99)00316-9

García-Ruiz, J. M. (2010). The Effects of Land Uses on Soil Erosion in Spain: A Review. *Catena*, *81*(1), 1–11. https://doi.org/10.1016/j.catena.2010.01.001

García-Ruiz, J. M., & Lana-Renault, N. (2011). Hydrological and erosive consequences of farmland abandonment in Europe, with special reference to the Mediterranean region—a review. *Agriculture, Ecosystems and Environment*, *140*, 317–338. https://doi.org/10.1016/j.agee.2011.01.003

Gaspar, L., Lizaga, I., Blake, W. H., Latorre, B., Quijano, L., & Navas, A. (2019). Fingerprinting changes in source contribution for evaluating soil response during an exceptional rainfall in Spanish pre-pyrenees. *Journal of Environmental Management*, *240*, 136–148. https://doi.org/10.1016/j.jenvman.2019.03.109

Gburek, W. J., & Sharpley, A. N. (1998). Hydrologic controls on phosphorus loss from upland agricultural watersheds. *Journal of Environmental Quality*, *27*, 267–277. https://doi.org/10.2134/jeq1998.00472425002700020005x

Gérard, F. (2016). Clay minerals, iron/aluminum oxides, and their contribution to phosphate sorption in soils—a myth revisited. *Geoderma*, *262*, 213–226. https://doi.org/10.1016/j.geoderma.2015.08.036

Ghafari, H., Gorji, M., Arabkhedri, M., Roshani, G. A., Heidari, A., & Akhavan, S. (2017). Identification and prioritization of critical erosion areas based on onsite and offsite effects. *Catena*, *156*, 1–9. https://doi.org/10.1016/j.catena.2017.03.014

Granger, S. J., Harris, P., Upadhayay, H. R., Sint, H., Pulley, S., Stone, M., Krishnappan, B. G., & Collins, A. L. (2021). Novel approaches to investigating spatial variability in channel bank total phosphorus at the catchment scale. *Catena*, *202*, 105223. https://doi.org/10.1016/j.catena.2021.105223

Hosseinzadehtalaei, P., Tabari, H., & Willems, P. (2020). Climate change impact on short-duration extreme precipitation and intensity–duration–frequency curves over Europe. *Journal of Hydrology*, *590*, 125249. https://doi.org/10.1016/j.jhydrol.2020.125249

Jin, K., Cornelis, W. M., Schiettecatte, W., Lu, J. J., Cai, D. X., Jin, J. Y., De Neve, S., Hartmann, R., & Gabriels, D. (2009). Effects of different soil management practices on total P and Olsen-P sediment loss: A field rainfall simulation study. *Catena*, *78*, 72–80. https://doi.org/10.1016/j.catena.2009.02.019

Joel, A., Wesström, I., Strock, J., & Messing, I. (2012). Method for in situ measurements of water, sediment and phosphorous transport in the upper soil profile. *Acta Agriculturae Scandinavica, Section B—Soil & Plant Science*, *62*, 252–259. https://doi.org/10.1080/09064710.2012.714399

Kaup, B. S., & Carter, B. J. (1987). Determining Ti source and distribution within a Paleustalf by micromorphology, submicroscopy and elemental analysis. *Geoderma*, *40*, 141–156. https://doi.org/10.1016/0016-7061(87)90019-X

Kharin, V. V., Zwiers, F. W., Zhang, X., & Hegerl, G. C. (2007). Changes in temperature and precipitation extremes in the IPCC Ensemble of Global Coupled Model Simulations. *Journal of Climate*, *20*, 1419–1444. https://doi.org/10.1175/JCLI4066.1

Kuhn, N. J., Armstrong, E. K., Ling, A. C., Connolly, K. L., & Heckrath, G. (2012). Interrill erosion of carbon and phosphorus from conventionally and organically farmed Devon silt soils. *Catena*, *91*, 94–103. https://doi.org/10.1016/j.catena.2010.10.002

Lasanta, T., Nadal-Romero, E., Errea, P., & Arnáez, J. (2016). The effect of landscape conservation measures in changing landscape patterns: A case study in Mediterranean Mountains. *Land Degradation and Development*, *27*, 373–386. https://doi.org/10.1002/ldr.2359

LECO (1996). *CNS-2000 elemental analyser – instruction manual*. LECO Corp.

Lima, P. L. T., Silva, M. L. N., Quinton, J. N., Armstrong, A., Inda, A. V., Batista, P. V. G., Poggere, G. C., & Curi, N. (2020). Tracing the origin of reservoir sediments using magnetic properties in southeastern Brazil. *Semina Ciencias Agrarias*, *41*, 847–864. https://doi.org/10.5433/1679-0359.2020v41n3p847

Lizaga, I., Gaspar, L., Blake, W. H., Latorre, B., & Navas, A. (2019). Fingerprinting changes of source apportionments from mixed land uses in stream sediments before and after an exceptional rainstorm event. *Geomorphology*, *341*, 216–229. https://doi.org/10.1016/j.geomorph.2019.05.015

Lizaga, I., Gaspar, L., Latorre, B., & Navas, A. (2020). Variations in transport of suspended sediment and associated elements induced by rainfall and agricultural cycle in a Mediterranean agroforestry catchment. *Journal of Environmental Management*, *272*, 111020. https://doi.org/10.1016/j.jenvman.2020.111020

Lizaga, I., Quijano, L., Palazón, L., Gaspar, L., & Navas, A. (2018). Enhancing connectivity index to assess the effects of land use changes in a Mediterranean catchment. *Land Degradation and Development*, *29*, 663–675. https://doi.org/10.1002/ldr.2676

Ma, X., Li, Y., Li, B., Han, W., Liu, D., & Gan, X. (2016). Nitrogen and phosphorus losses by runoff erosion: Field data monitored under natural rainfall in three gorges reservoir area, China. *Catena*, *147*, 797–808. https://doi.org/10.1016/j.catena.2016.09.004

Magiera, T., Strzyszcz, Z., Kapicka, A., & Petrovsky, E. (2006). Discrimination of lithogenic and anthropogenic influences on topsoil magnetic susceptibility in Central Europe. *Geoderma*, *130*, 299–311. https://doi.org/10.1016/j.geoderma.2005.02.002

McDowell, R., Sharpley, A., & Folmar, G. (2001). Phosphorus export from an agricultural watershed: Linking source and transport mechanisms. *Journal of Environmental Quality*, *30*, 1587–1595. https://doi.org/10.2134/jeq2001.3051587x

Messing, I., Joel, A., Wesström, I., & Strock, J. (2015). Influence of higher rain intensities on phosphorus movements in the upper half meter of macroporous clay soil. *Acta Agriculturae Scandinavica, Section B—Soil & Plant Science*, *65*, 93–99. https://doi.org/10.1080/09064710.2014.996588

Nadal-Romero, E., Rodríguez-Caballero, E., Chamizo, S., Juez, C., Cantón, Y., & García-Ruiz, J. M. (2022). Mediterranean badlands: Their driving processes and climate change futures. *Earth Surface Processes and Landforms*, *47*, 17–31. https://doi.org/10.1002/esp.5088

Navas, A., López-Vicente, M., Gaspar, L., Palazón, L., & Quijano, L. (2014). Establishing a tracer-based sediment budget to preserve wetlands in Mediterranean mountain agroecosystems (NE Spain). *Science of the Total Environment*, *496*, 132–143. https://doi.org/10.1016/j.scitotenv.2014.07.026

Navas, A., Quine, T. A., Walling, D. E., Gaspar, L., Quijano, L., & Lizaga, I. (2017). Relating intensity of soil redistribution to land use changes in abandoned Pyrenean fields using fallout Caesium-137. *Land Degradation & Development*, *28*, 2017–2029. https://doi.org/10.1002/ldr.2724

Neidhardt, H., Achten, F., Kern, S., Schwientek, M., & Oelmann, Y. (2019). Phosphorus pool composition in soils and sediments of transitional ecotones under the influence of agriculture. *Journal of Environmental Quality*, *48*, 1325–1335. https://doi.org/10.2134/jeq2019.01.0012

Novotny, V., & Chesters, G. (1989). Delivery of sediment and pollutants from nonpoint sources: A water quality perspective. *Journal of Soil And Water Conservation*, *44*, 568–576.

Otero, J. D., Figueroa, A., Muñoz, F. A., & Peña, M. R. (2011). Loss of soil and nutrients by surface runoff in two agro-ecosystems within an Andean paramo area. *Ecological Engineering*, *37*, 2035–2043. https://doi.org/10.1016/j.ecoleng.2011.08.001

Quijano, L., Chaparro, M. A. E., Marié, D. C., Gaspar, L., & Navas, A. (2014). Relevant magnetic and soil parameters as potential indicators of soil conservation status of Mediterranean agroecosystems. *Geophysical Journal International*, *198*(3), 1805–1817. https://doi.org/10.1093/gji/ggu239

Quinton, J. N., Catt, J. A., & Hess, T. M. (2001). The selective removal of phosphorus from soil: Is event size important? *Journal of Environmental Quality*, *30*, 538–545. https://doi.org/10.2134/jeq2001.302538x

Ramos, M. C., Benito, C., & Martínez-Casasnovas, J. A. (2015). Simulating soil conservation measures to control soil and nutrient losses in a small, vineyard dominated, basin. *Agriculture, Ecosystems and Environment*, *213*, 194–208. https://doi.org/10.1016/j.agee.2015.08.004

Ramos, M. C., & Durán, B. (2014). Assessment of rainfall erosivity and its spatial and temporal variabilities: Case study of the Penedès area (NE Spain). *Catena*, *123*, 135–147. https://doi.org/10.1016/j.catena.2014.07.015

Ramos, M. C., Lizaga, I., Gaspar, L., & Navas, A. (2022). The impacts of exceptional rainfall on phosphorus mobilisation in a mountain agroforestry catchment (NE, Spain). *Catena*, *216*, 106407. https://doi.org/10.1016/j.catena.2022.106407

Ramos, M. C., Lizaga, I., Gaspar, L., Quijano, L., & Navas, A. (2019). Effects of rainfall intensity and slope on sediment, nitrogen and phosphorous losses in soils with different use and soil hydrological properties. *Agricultural Water Management*, *226*, 105789. https://doi.org/10.1016/j.agwat.2019.105789

Ramos, M. C., & Martínez-Casasnovas, J. A. (2009). Impacts of annual precipitation extremes on soil and nutrient losses in vineyards of NE Spain. *Hydrological Processes*, *23*, 224–235. https://doi.org/10.1002/hyp.7130

Ramos, M. C., Nacci, S., & Pla, I. (2000). Soil sealing and its influence on erosion rates for some soils in the Mediterranean area. *Soil Science*, *165*, 398–403. https://doi.org/10.1097/00010694-200005000-00003

Räty, M., Järvenranta, K., Saarijärvi, E., Koskiaho, J., & Virkajärvi, P. (2020). Losses of phosphorus, nitrogen, dissolved organic carbon and soil from a small agricultural and forested catchment in east-Central Finland. *Agriculture, Ecosystems and Environment*, *302*, 107075. https://doi.org/10.1016/j.agee.2020.107075

Sanjari, S., Farpoor, M. H., & Mahmoodabadi, M. (2021). Magnetic susceptibility of soils as affected by lithology, geomorphology and climate in Jazmoorian watershed, Central Iran. *Geosciences Journal*, *25*, 903–913. https://doi.org/10.1007/s12303-021-0007-5

Sharpley, A. N., Kleinman, P. J. A., Heathwaite, A. L., Gburek, W. J., Folmar, G. J., & Schmidt, J. P. (2008). Phosphorus loss from an agricultural watershed as a function of storm size. *Journal of Environmental Quality*, *37*, 362–368. https://doi.org/10.2134/jeq2007.0366

Shigaki, F., Sharpley, A., & Prochnow, L. I. (2007). Rainfall intensity and phosphorus source effects on phosphorus transport in surface runoff from soil trays. *Science of the Total Environment*, *373*, 334–343. https://doi.org/10.1016/j.scitotenv.2006.10.048

Spohn, M. (2020). Phosphorus and carbon in soil particle size fractions: A synthesis. *Biogeochemistry*, *147*, 225–242. https://doi.org/10.1007/s10533-019-00633-x

Steegen, A., Govers, G., Nachtergaele, J., Takken, I., Beuselinck, L., & Poesen, J. (2000). Sediment export by water from an agricultural catchment in the Loam Belt of Central Belgium. *Geomorphology*, *33*, 25–36. https://doi.org/10.1016/S0169-555X(99)00108-7

Tian, X., Bing, H., Wu, Y., Zhu, H., Zhao, W., He, Q., & Xiong, D. (2022). Farmland abandonment decreases soil bioavailable phosphorus but increases organic phosphorus in the mid-hills of Nepal. *Catena*, *33*, 106000. https://doi.org/10.1016/j.catena.2021.106000

Udawatta, R. P., Motavalli, P. P., & Garrett, H. E. (2004). Phosphorus loss and runoff characteristics in three adjacent agricultural watersheds with claypan soils. *Journal of Environmental Quality*, *33*, 1709–1719. https://doi.org/10.2134/jeq2004.1709

Ulén, B. M., & Kalisky, T. (2005). Water erosion and phosphorus problems in an agricultural catchment—need for natural research for implementation of the EU water framework directive. *Environmental Science & Policy*, *8*, 477–484. https://doi.org/10.1016/j.envsci.2005.06.005

Vallebona, C., Pellegrino, E., Frumento, P., & Bonari, E. (2015). Temporal trends in extreme rainfall intensity and erosivity in the Mediterranean region: A case study in southern Tuscany, Italy. *Climate Change*, *128*, 139–151. https://doi.org/10.1007/s10584-014-1287-9

Wang, L., Yang, Y., Zheng, J., Liu, Y., Guo, Q., Wang, D., & Liu, B. (2017). Effects of fertilization on nitrogen and phosphorous losses from cropland in Beijing mountainous area: A case study on the Miyun reservoir watershed. *Journal of Soil and Water Conservation*, *15*, 97–104. https://doi.org/10.16843/j.sswc.2017.01.012

Wang, R., Cai, C., Zhang, J., Sun, S., & Zhang, H. (2022). Study on phosphorus loss and influencing factors in the water source area. *International Soil and Water Conservation Research*, *10*, 324–334. https://doi.org/10.1016/j.iswcr.2021.07.002

Xie, Y., Liu, B., & Nearing, M. A. (2002). Practical thresholds for separating erosive and non-erosive storms. *Transactions of the American Society of Agricultural Engineers*, *45*, 1843–1847. https://doi.org/10.13031/2013.11435

Yang, P., Mao, R., & Shao, H. (2009). An investigation on magnetic susceptibility of hazardous saline-alkaline soils from the contaminated Hai River basin, China. *Journal of Hazardous Materials*, *172*, 494–497. https://doi.org/10.1016/j.jhazmat.2009.07.011

Yang, X., Chen, X., & Yang, X. (2019). Effect of organic matter on phosphorus adsorption and desorption in a black soil from Northeast China. *Soil and Tillage Research*, *187*, 85–91. https://doi.org/10.1016/j.still.2018.11.016

Yuan, Y., & Koropeckyj-Cox, L. (2022). SWAT model application for evaluating agricultural conservation practice effectiveness in reducing phosphorous loss from the Western Lake Erie Basin. *Journal of Environmental Management*, *302*, 114000. https://doi.org/10.1016/j.jenvman.2021.114000

Zimmer, D., Kahle, P., & Baum, C. (2016). Loss of soil phosphorus by tile drains during storm events. *Agricultural Water Management*, *167*, 21–28. https://doi.org/10.1016/j.agwat.2015.12.017

How to cite this article: Ramos, M. C., Lizaga, I., Gaspar, L., & Navas, A. (2023). Particulate phosphorus in runoff in a Mediterranean agroforestry catchment driven by land use and rainfall characteristics. *Land Degradation & Development*, *34*(16), 4882–4896. https://doi.org/10.1002/ldr.4816